Intercalibration of multiple thermochonometric systems at the Little Devil's Postpile contact aureole

David L Shuster — Dept. Earth and Planetary Science, UC Berkeley - dshuster@berkeley.edu
Peter W Reiners — Dept. Geosciences, University of Arizona
Leif Karlstrom — Dept. Geophysics, Stanford University
Jennifer L Schmidt — Dept. Earth and Environmental Sciences, Lehigh University
Peter K Zeitler — Dept. Earth and Environmental Sciences, Lehigh University
Richard A Ketcham — Dept. Geological Sciences, University of Texas, Austin

Summary *- A fundamental assumption in thermochronology is extrapolation of kinetic parameters over geologic timescales, temperatures, and mineral compositions that often differ significantly from the laboratory conditions used to quantify them. In this study, we aim to test and intercalibrate kinetic parametersof multiple thermochronometric systems using a tractable, natural thermal perturbation associated with the emplacement of a small, young basalt intrusion into granite in the Sierra Nevada, the site of the classic study of Calk and Naeser (1973). We collected a suite of samples along a linear transect orthogonal to the contact, from which the minerals apatite, zircon, titanite, epidote, magnetite, biotite, horneblende, K-feldspar, and plagioclase were separated. Our results to date reveal that the (U-Th)/He system in apatite was completely reset within ~7 m of the contact during basalt emplacement ~8 Ma. At distances >16 m from the contact, the apatite He ages are uniformly ~58 Ma, which likely represents the background (i.e., unperturbed) cooling ages of the granite. Apatite $^{4}He/^{3}He$ thermochronometry and an observed transition from background- to rest-ages of these samples are quantitatively consistent with a higher degree of thermal perturbation nearer to the contact. As predicted by our current quantification of radiation damage accumulation influence on He diffusion kinetics (Flowers et al, 2009), we observe correlation between the "effective uranium" concentration and He ages of individual apatite crystals, particularly within this transition zone. In contrast, the (U-Th)/He system in zircon is only partially reset ~7 m from the contact, and the background cooling ages at distances >10 m are ~78 Ma, consistent with a $^{40}Ar/^{39}Ar$ age-spectrum from a distal K-feldspar that rises from ~70 to ~80 Ma; both observations are consistent with the relative, experimentally determined temperature sensitivities of these minerals. We present ongoing numerical modeling that provides a framework with which to quantitatively compare and assess these results with forthcoming $^{40}Ar/^{39}Ar$ and fission track results in various mineral systems. Inversion of data using these multi-material conductive models will be used to assess the sensitivity of results to assumptions about geometry (1D, 2D, 3D), duration of basalt emplacement, and pre-intrusion cooling rate.*

Little Devil's Postpile, Yosemite National Park, California

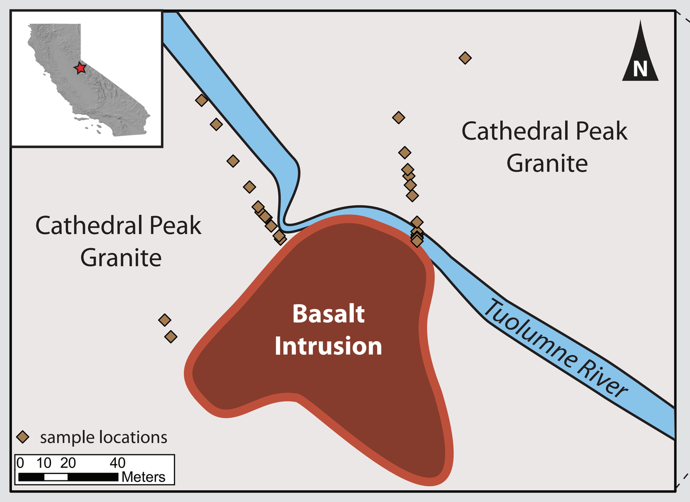

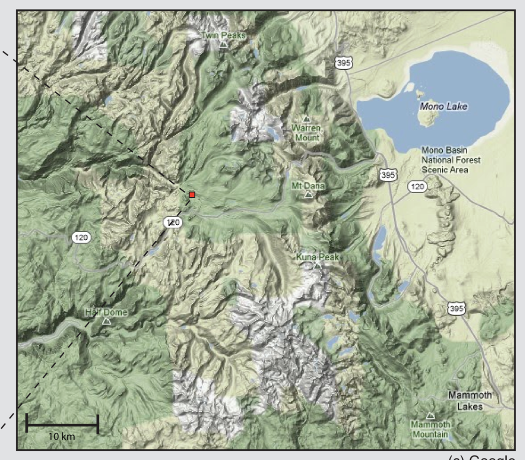

Located within Yosemite National Park near Tuolumne Meadows, the Little Devil's Postpile is a porphyritic olivine basalt that intruded into the Cathedral Peak Granite batholith, a Cretaceous porphyritic quartz monzonite. The basalt intrusion is irregularly shaped, approximately 100 m in cross-section. Previous work revealed apatite fission track (AFT) ages of ~8 Ma near the contact, providing constraint on the timing of intrusion (Calk and Naeser, 1973). We collected bedrock samples granite along two transects from the contact and samples of the basalt itself. Our objective is to use the thermal perturbation associated with basalt emplacement to test lab-based kinetic parameters for different parent-daughter thermochronology systems in different minerals, both in the absolute and relative to one another.

Expected thermal scenario and previous work

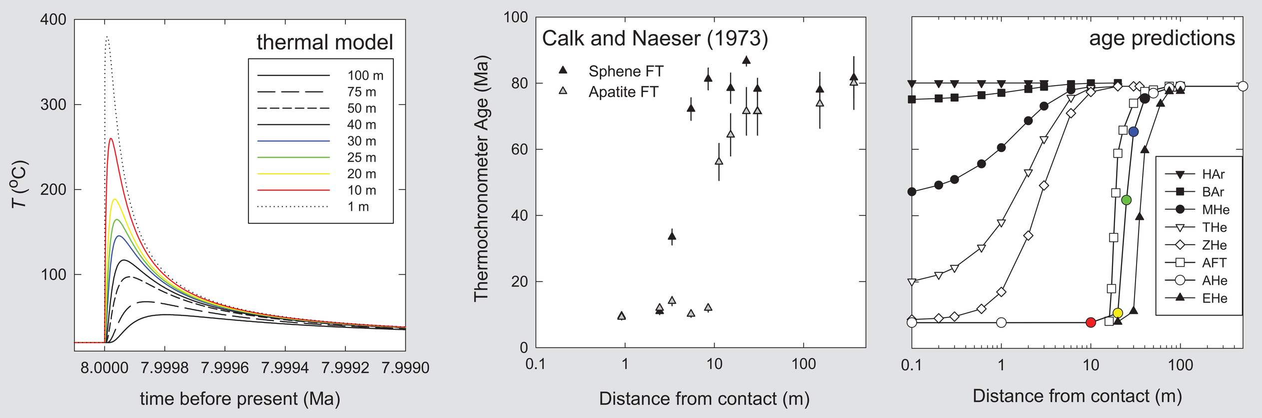

The basic thermal setting of LDP. The Cathedral Peak Granite crystalized at ~88 Ma (Bateman and Chappell, 1979) We expect the granite to have resided at relatively low temperatures for a long duration (10s of Ma) prior to the basalt emplacement at ~8 Ma. Over a brief timescale during the intrusion, the surrounding granite bedrock would have experienced a pulse in temperature due to conduction of heat from the basalt, with maximum temperatures primarily controlled by distance from the contact (left panel). We therefore expect thermochronological systems to be more extensively reset (e.g., due to thermally activated diffusion) near the contact, and less perturbed far from the contact. Calk and Naeser (1973) observed this general pattern in both the apatite and zircon fission track systems (middle panel). Given the large number of mineral systems present in the granite, the thermal perturbation can be used to make predictions of observables for both established, and developing thermochronological systems (right panel).

Citations

Bateman, P.C., Chappell, B.W., **(1979)** Crystallization, fractionation, and solidification of the Tuolumne intrusive series, Yosemite National Park, California. *Geological Society of America Bulletin* 90, 465-482
Calk, L.C., Naeser, C.W., **(1973)** The thermal effect of a basalt intrusion on fission tracks in quartz monzonite. *The Journal of Geology*, 189-198
Flowers, R.M., Ketcham, R.A., Shuster, D.L., Farley, K.A., **(2009)** Apatite (U-Th)/He thermochronometry using a radiation damage accumulation and annealing model. *Geochimica et Cosmochimica Acta* 73, 2347-2365
Harrison, T.M., Grove, M., Lovera, O.M., Zeitler, P.K., **(2005)** Continuous thermal histories from inversion of closure profiles. *Reviews in mineralogy and geochemistry* 58, 389-409
Karlstrom, L., Dufek, J., Manga, M., **(2010)** Magma chamber stability in arc and continental crust. *Journal of Volcanology and Geothermal Research* 190, 249-270
Lovera, O.M., Grove, M., Mark Harrison, T., Mahon, K., **(1997)** Systematic analysis of K-feldspar $^{40}Ar^{39}Ar$ step heating results: I. Significance of activation energy determinations. *Geochimica et Cosmochimica Acta* 61, 3171-3192
Lovera, O.M., Richter, F.M., Harrison, T.M., **(1989)** The $^{40}Ar/^{39}Ar$ Thermochronometry for Slowly Cooled Samples. Journal of Geophysical Research 94, 17,917-917,935
Shuster, D.L., Flowers, R.M., Farley, K.A., **(2006)** The influence of natural radiation damage on helium diffusion kinetics in apatite. *Earth and Planetary Science Letters* 249, 148-161
Zeitler, P.K., **(2004)** Arvert 4.1. Inversion of $^{40}Ar/^{39}Ar$ age spectra. Users manual (http://www.ees.lehigh.edu/EESdocs/geochron/downloads/arvert/arvert_41_manual.pdf)

This work is supported by the Petrology and Geochemistry program of the US National Science Foundation.
Field work could not have been completed without the assistance of Yosemite National Park and Dr. Greg Stock.

(U-Th)/He system in apatite and zircon

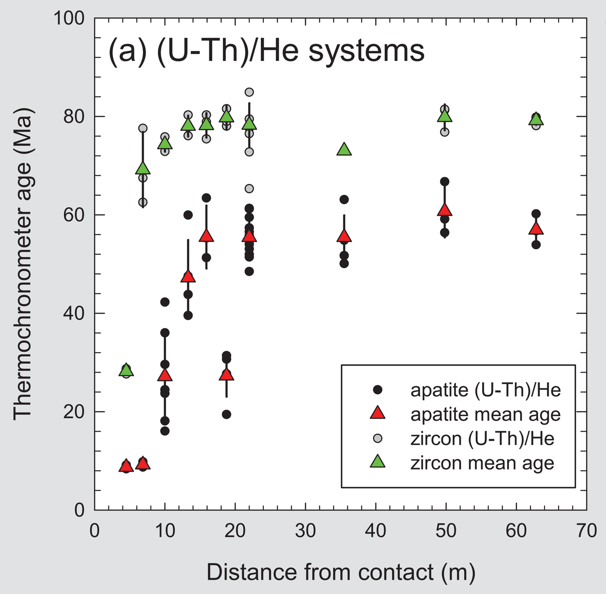

Apatite and zircon (U-Th)/He ages (individual crystal ages and mean ages). As expected from differences in kinetics of He diffusion, zircon He ages are systematically older at all sample locations. Somewhat unexpectedly, we find a large difference in the background cooling ages indicating relatively slow cooling between 58-78 Ma, or influece of the intrusion on apatite He ages very far from the contact. Both systems show a transition between background cooling age and complete resetting at the timing of intrusion (~8 Ma).

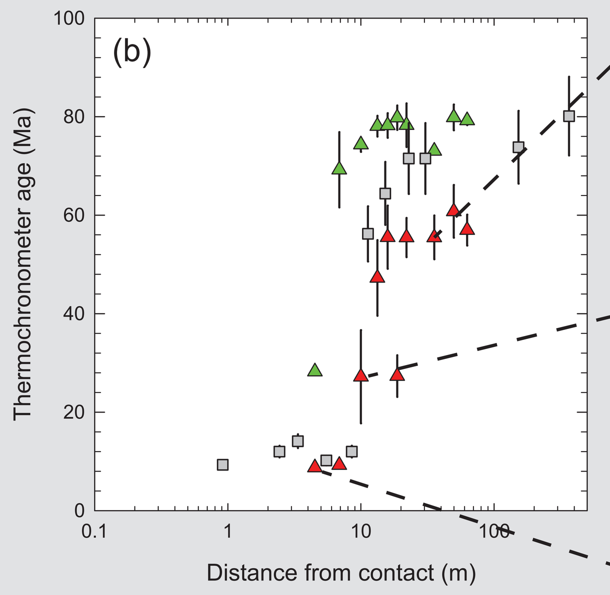

$^{4}He/^{3}He$ thermochronometry

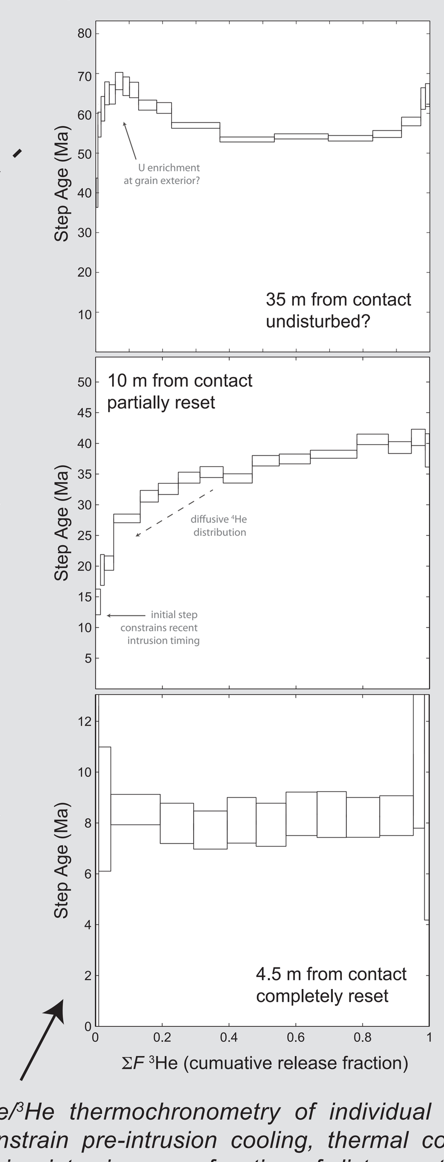

$^{4}He/^{3}He$ thermochronometry of individual apatites constrain pre-intrusion cooling, thermal conditions during intrusion as a function of distance, timing of the intrusion and post-intrusion cooling. Samples near the contact (e.g., 4.5 m) are consistent with 100% loss of pre-intrusion ^{4}He, followed by rapid cooling to low-T (i.e., a flat age spectrum). Samples in the transition zone (e.g., 10 m) reflect partial diffusive loss of ^{4}He during intrusion. In the example shown, the initial step age constrains an upper bound the timing of temperature increase (<12 Ma). ^{4}He in far samples (e.g., 35) appear not to have been influenced by the intrusion; the example shown has evidence of higher U near the crystal edge.

Partially reset apatites (U-Th)/He age - eU correlation

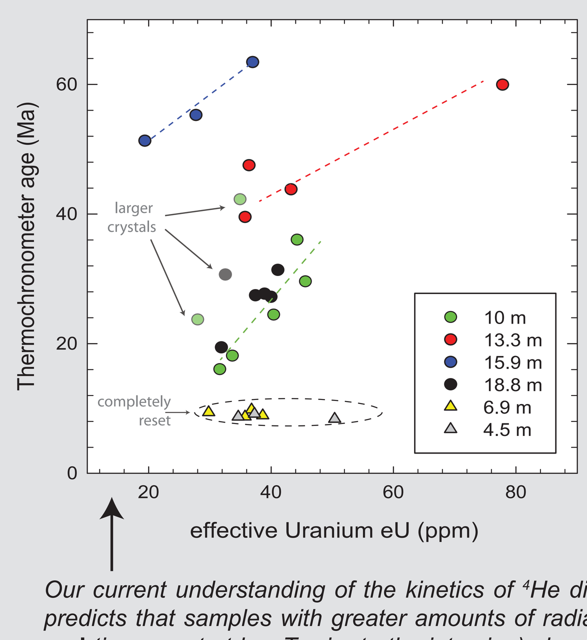

Our current understanding of the kinetics of ^{4}He diffusion in apatite (Shuster et al., 2006, Flowers et al., 2009) predicts that samples with greater amounts of radiation damage (due to higher U plus Th, or eU, concentration ***and*** *time spent at low-T prior to the intrusion) should be less susceptible to heating than samples with lower eU. As expected, at locations where samples experienced partial ^{4}He loss, we find correlation between the eU and (U-Th)/He age of individual apatite crystals. However, samples within 6.9 m from the contact do not show correlation, indicating that the intrusion temperatures were sufficiently high at these locations to completely reset all samples, regardless of the radiation damage effect on He diffusion.An expected crystal size effect is also observed, with larger crystals less influenced by heating.*

Thermal model of the intrusion

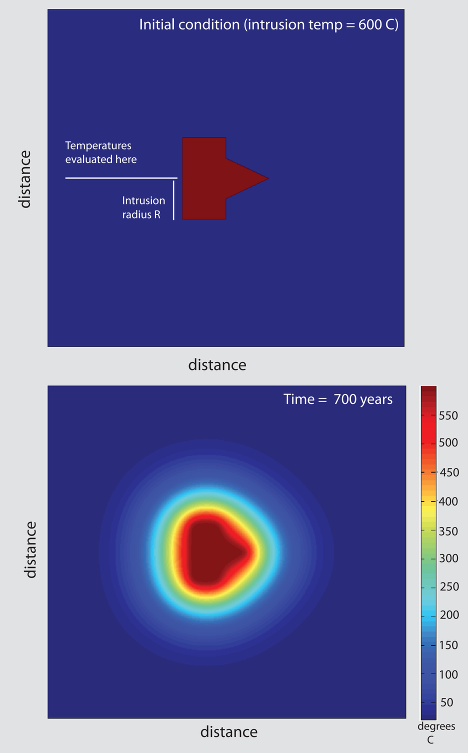

We use the thermal model of Karlstrom et al 2010 JVGR to constrain the intrusion processes responsible for generating thermochronological data. This model solves conservation of enthalpy in two dimensions with a finite volume method for a two-component system (intruding basalt with 2 wt pct water, tonalite surrounding, modeled by distinct melt-fraction temperature curves), keeping track of latent heat and relative melt fractions of the components. This model will eventually be used to cross-calibrate different chronometers. Initial work focuses on He apatite data, and model sensitivity.

We use a geometry that approximates the outcrop dimensions of the intrusion. However, because points only 10 m away from the contact are not completely reset (i.e., did not experience temperatures in excess of 300 C) we find that the model intrusion must either be (I) much smaller than the outcrop (by about an order of magnitude in radius) or (ii) cooler than the basalt solidus (advection through the plug or by hydrothermal fluids cools the intrusion faster than conduction).

Our best fitting model so far has intrusion radius R=5 m, an intrusion duration (constant temperature boundary condition) of 8.4 hours, and an intrusion temperature at the solidus of 600 C. The model is very sensitive to radius, slightly less sensitive to duration of flow through intrusion and less to intrusion boundary temperature. We hope to tune these three parameters along with the background cooling rate to match thermochronologic data.

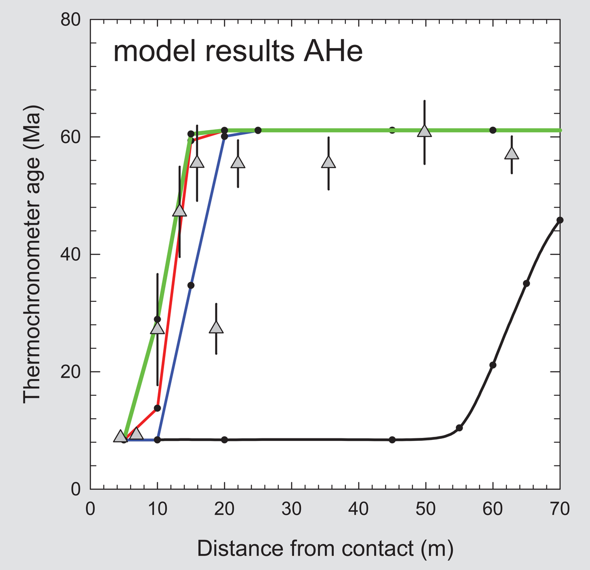

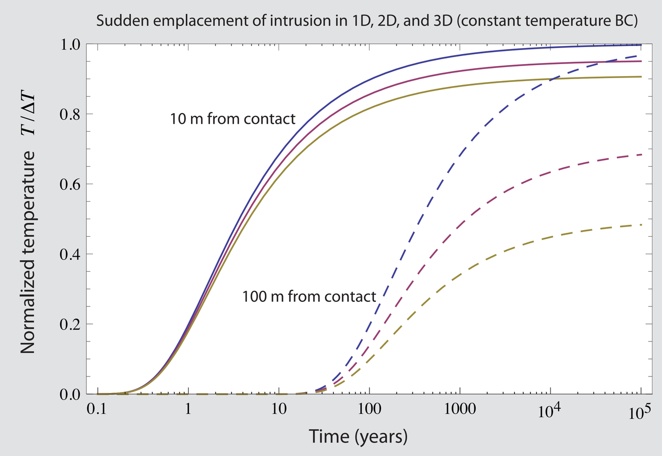

Effect of geometery
Our 2D thermal model will well represent the time-temperature pathways of the country rocks surrounding the intrusion in the near field even if the true geometry is quite complex. Because the transition to reset He ages occurs in the near field, we are confident that dimensionality effects play little role. However, in the far field (distance >> radius) there are significant difference between the thermal evolution of 1D, 2D, 3D intrusions, as illustrated by these representative analytic solutions.

$$T_{1D} = \Delta T \, erfc\left(\frac{r-R}{2\sqrt{\kappa t}}\right) \quad \text{Plane}$$

$$T_{2D} = \Delta T \sqrt{\frac{R}{r}} \, erfc\left(\frac{r-R}{2\sqrt{\kappa t}}\right) \quad \text{Cylinder (approximate solution)}$$

$$T_{3D} = \Delta T \frac{R}{r} \, erfc\left(\frac{r-R}{2\sqrt{\kappa t}}\right) \quad \text{Sphere}$$

$^{40}Ar/^{39}Ar$ thermochronometry

Distal Sample (22 m) Kinetics and Inverse Model

K-feldspar MDD inversion model for thermal history (Lovera et al.,1989) based on $^{40}Ar/^{39}Ar$ age spectrum for distal sample located 22 meters from the intrusion, and using apatite U-Th/He data as an additional constraint. This thermal history that should have been shared by all samples in the area prior to emplacement of the basalt plug. Inversions performed using the Arvert 4.1 controlled-random search code (Harrison et al., 2005; Zeitler, 2004).

(a)

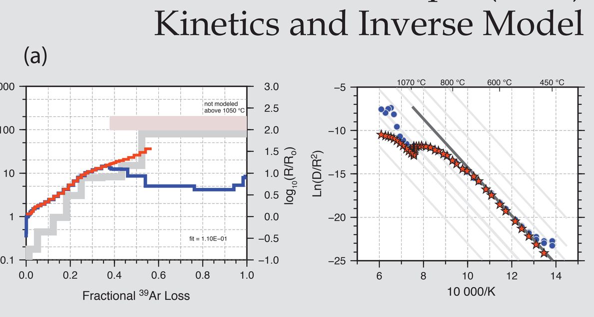

SAMPLE: stepheat.s
Using steps 10 to 17:
E = 55.47 ± 0.48 kcal/mol
$Log_{10}(D/R_o^2)$ = 5.951 ± 0.123
Unweighted regression

9 domains:

N	Vol.	Vol_T	Rel. Size
1	0.014	0.01	0.04
2	0.038	0.05	0.18
3	0.071	0.12	0.44
4	0.060	0.18	0.95
5	0.066	0.25	3.04
6	0.093	0.34	7.85
7	0.090	0.43	8.26
8	0.091	0.52	14.95
9	0.476	1.00	80.24

(a) Arrhenius and $log(R/R_o)$ plots summarizing the diffusion-domain model used in inversion runs (obtained using modified code based on Oscar Lovera's domain-finding routine autoarr (Lovera et al., 1997). Blue points and R/R_o spectrum – observed data. Red – model. Gray spectrum shows modeled diffusion-domain spectrum. Table gives kinetic and domain results.

(b) Inverse model results. On both the temperature-history and age-spectrum plots, the green and red curves show, respectively, the 15 best-fit and 15 worst-fit models to the age spectrum, following model completion. On the thermal-history plots, the dark gray curves show the envelopes for the better-fitting data (these envelopes are not solutions). For age spectrum, only the portion shown in blue was modeled.

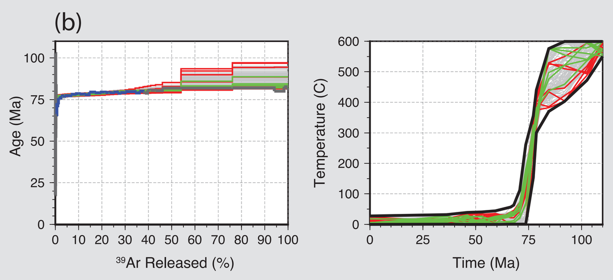

Proximal Sample (4.5 m) Kinetics and Forward Model

Results for proximal sample located 4.5 meters from the intrusion.

(a)

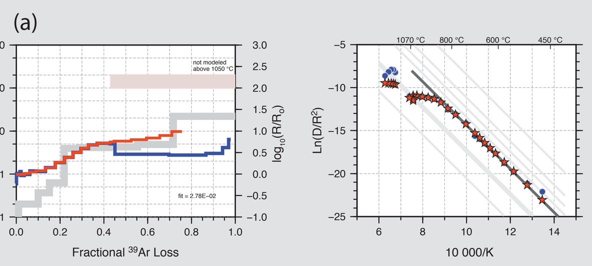

SAMPLE: LDP1005
Using steps 3 to 11:
E = 50.38 ± 1.12 kcal/mol
$Log_{10}(D/R_o^2)$ = 4.775 ± 0.267
Unweighted regression

9 domains:

N	Vol.	Vol_T	Rel. Size
1	0.011	0.01	0.05
2	0.089	0.10	0.20
3	0.051	0.15	0.37
4	0.068	0.22	0.62
5	0.070	0.29	3.96
6	0.135	0.42	4.10
7	0.130	0.55	4.27
8	0.163	0.72	4.88
9	0.283	1.00	21.93

(a) Kinetic and domain structure, marked as in previous figure.

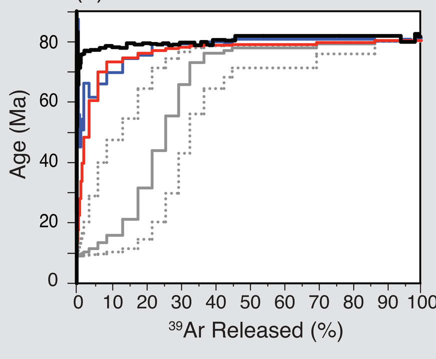

(b) Forward model results showing age spectra calculated using the sample's domain structure and a distance-appropriate thermal thermal history taken from those published by Calk and Naeser (1973). Black – measured spectrum from distal sample at 22 meters (for reference; above); Blue – measured spectrum from reset sample at 4.5 m; Gray – predicted spectrum based on Calk and Naeser (1973) thermal model (maximum temperature 521 ˚C; duration of pulse on order 10 years); Gray dashed – predicted spectrum for maximum temperatures offset 100 ˚C below Calk and Naeser model. The better fit for the cooler model is consistent with the very high effective magma temperature of 1530 ˚C used by Calk and Naeser (1973) to account for latent heat; such an approximation is not accurate for regions near the intrusive contact.